



e-ISSN: 2319-8753 | p-ISSN: 2347-6710

IJRSET

International Journal of Innovative Research in
SCIENCE | ENGINEERING | TECHNOLOGY

INTERNATIONAL JOURNAL OF INNOVATIVE RESEARCH

IN SCIENCE | ENGINEERING | TECHNOLOGY

Volume 12, Issue 2, February 2023

ISSN INTERNATIONAL
STANDARD
SERIAL
NUMBER
INDIA

Impact Factor: 8.118

 9940 572 462

 6381 907 438

 ijirset@gmail.com

 www.ijirset.com

An Optimum Multilayer Perceptron Based Neural Network for Stator Inter-Turn and Eccentricity Fault Detection and Classification in Three-Phase Permanent Magnet Synchronous Motor

P.G. Asutkar¹, Dr. Z.J. Khan²

Assistant Professor, Department of Electrical Engineering, RCERT, Chandrapur, (M.H) India¹

Principal & Professor, Department of Electrical Engineering, RCERT, Chandrapur, (M.H) India²

ABSTRACT: Permanent Magnet Synchronous Motors (PMSMs) are subjected to various operating, environmental, and other conditions, due to which incipient fault occurs. If these faults are undetected leads to catastrophic failure. For reliable and safe operation of PMSM. Online condition monitoring, fault detection, and diagnosis were required. Many researchers proposed various techniques for fault detection and diagnosis, which requires good domain knowledge and costly types of equipment. This paper proposed an optimal multilayer perceptron (MLP) neural network and principal component analysis (PCA) for dimensional reduction of input space. Two faults are created on three-phase permanent magnet synchronous motor stator inter-turn and eccentricity on varying load conditions from the no-load rated load, and greater than the rated load. The experimental data is generated on 1 hp, 3 phase, 4 poles, and 1500 rpm permanent magnet synchronous motor during healthy and faulty conditions. Various sensors are inbuilt internally and externally into the PMSM motor for the measurement of different parameters. 12 different measurable parameters include three-phase motor intake current, three-phase motor applied voltage, power factor, winding temperatures, and bearing sound. The proposed classifier with 12 input parameters is designed and verified for optimal performance in fault identification and classification, nearly 100% classification accuracy is achieved.

KEYWORDS: Permanent Magnet Synchronous Motor (PMSMs), Fault Diagnosis, Fault Classifications, Stator inter-turn, Eccentricity, Multilayer Perceptron (MLP), Principal Component Analysis (PCA).

I. INTRODUCTION

Permanent Magnet Synchronous Motor (PMSMs) is widely used in commercial and industrial applications in a broad power range from mW to MW. The use of a permanent magnet in the construction of a motor brings the following benefits compared to other electric motors, high torque to weight ratio, better dynamic performance, and high efficiency because rotor loss is negligible and simple in construction and maintenance.[1] The applications of PMSM includes industry, public life, defense force, aerospace, and transportation system.[2] PMSMs are generally reliable and robust because of the electrical and mechanical symmetry between the rotor and stator. However, due to fundamental limitations of a material lifetime, deterioration, manufacturing defects, environmental conditions, working conditions, loading conditions, and continuous operation of the motor an unexpected failure occurs which leads to an incipient fault that, if undetected turns to catastrophic failure which in turn loss of production, loss of valuable human life and are cost-effective.[3,4] To maintain the electric motor in good working conditions. Online condition monitoring, fault detection, and diagnosis are required.[5]

Faults in PMSMs are categorized into three parts Electrical, Mechanical, and Magnetic. Electric faults include stator-related faults such as inter-turn winding short circuits, the opening of one or more phases of the stator, phase-to-ground fault, insulation degradation, and electronics drive failure.[6] Mechanical faults include a bent shaft, bearing defect, and eccentricity. Magnetic faults consist of the demagnetization of the permanent magnet and broken rotor defect. According to electric power research (EPRI) and an IEEE survey.[7]



Table .1 Fault occurrence

Survey Report	Bearing related fault	Stator related fault	Rotor related fault	Others
EPRI	41%	38%	10%	12%
IEEE	40%	38%	08%	22%

According to scrupulous reviews, many researchers have developed many tools and techniques for incipient faults, detection, and diagnosis. All these techniques come under the following broad categories, signal-based fault detection technique, machine theory-based fault analysis, simulation-based fault analysis, and model-based fault diagnosis technique. Electric fault involves stator-related faults are one of the most frequent related faults in three-phase PMSM motors. This occurs due to the degradation of insulating material turns into an inter-turn fault which increases the torque ripples in the motor and leads to stator inter-turn[8]. The inter-turn circulates a large current in the stator winding causing excessive heat in the winding, which creates phase-to-phase and phase-to-ground faults. If this fault is undetected, turn to motor repair as the PMSM motor is costly. Many researchers have proposed various techniques for stator inter-turn fault detection and diagnosis, such as motor current signature analysis (MCSA),[9] winding function theory (WFT), modified winding function theory (MWFT),[10] finite element analysis based on continuous wavelet transform, discrete wavelet transform and wavelet analysis, time-step finite element method (FEM) by using a magnetic field, 2D-step finite element method for dynamic modeling, 2D-FEM simulation to study magnetic effect due to temperature rise, zero, positive and negative sequence components of current and voltage to detect stator inter-turn.[11]

Mechanical faults consist of bearing and eccentricity, bearing faults occur due to inner raceway, outer raceway, ball damage, and misalignment of bearing. eccentricity faults are categorized as static eccentricity (SE), dynamic eccentricity (DE), and mixed eccentricity (ME).[12] Eccentricity in three-phase PMSM is caused due to a manufacturing defect, unbalanced mass shaft, and bearing defect which may cause air gap irregularity between stator and rotor with additional vibration, noise, and torque pulsation, resulting in unbalanced magnetic pull (UMP). These types of faults are diagnosed by the time-stepping finite method which takes the geometrical and physical characteristics of machines.[13] Fast Fourier transformation is used for the analysis of split phase current, Field reconstruction method is a way used to study torque pulsation and acoustic noise. Motor current signature is used to detect frequency components in the line current spectra. 2D finite element analysis to detect stator current-induced harmonics and dynamic air gap.[14]

II. FAULT CLASSIFICATION USING ANN

The following procedure is proposed for fault detection and classification.

- FAULT CREATED ON PMSM.
- DATA GENERATION AND COLLECTION.
- DATA SELECTION.
- FAULT CLASSIFICATION.

A. Fault Created on Permanent Magnet Synchronous Motor.

This paper proposed two faults created on permanent magnet synchronous motor, stator inter-turn (IT) and eccentricity. Eccentricity is categorized into three parts namely static eccentricity (SE), dynamic eccentricity (DE), and mixed eccentricity (ME). For creating a Fault PMSM motor of 1 hp, three-phase, 4 poles, 1500 rpm, 415 V, 50 Hz is used.

1. Stator inter-turn fault.

To create the effect of stator inter-turn fault in a three-phase PMSM motor. The main R-phase winding has been modified by taking out six tapping for shorting. Without disturbing the remaining two phases. After every two turns one tapping is taken out 2,4,6,8,10,12. The additional extra wires of very small distance are attached to the end turn and the other end of these external wires is attached to the designed chromium sheet near the motor terminal.

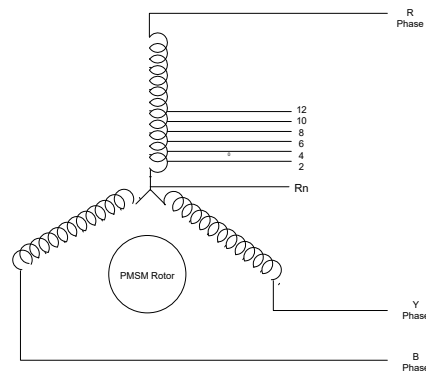


Fig.1 Electrical model of Stator inter-turn

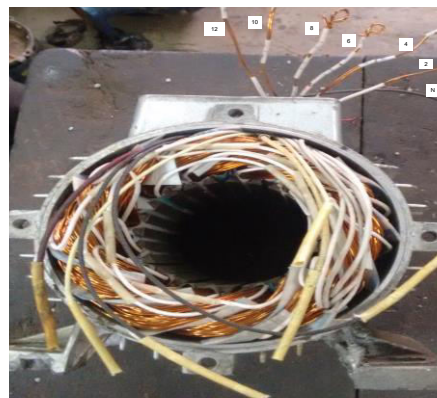


Fig.2 Stator of PMSM with stator iinter-turn.

Fig.2 shows the setup of 24 stator slots of three-phase winding with stator inter-turn tapping.

Table 2. Data of stator inter-turn fault

Turn shorted	0-2	0-4	0-6	0-8	0-10	0-12
R (Ω)	0.0734	0.1474	0.1902	0.2598	0.4454	0.6482
L (μ H)	4.5 μ H	15.8	34.4	54.8	128.3	156.8
Z (Ω)	0.0783	0.1643	0.2879	0.4291	0.9213	1.6625
θ	+21.06	+36.12	+45.82	+53.06	+61.07	+68.31

2. Eccentricity fault.

The eccentricity fault of the stator and rotor is mainly due to mechanical reasons. Machine eccentricity is the condition of the unequal air gap that exists between the stator and rotor.[15] When eccentricity becomes large the resulting unbalanced radial force can cause the stator to rotor rub which results in serious damage to the stator core and winding. In this fault symmetrical axis of the stator, the symmetrical axis of the rotor, and the rotating axis of the rotor are displaced from each other.[16] The static eccentricity fault rotor axis is shifted from the stator axis, the rotor turns around the rotor axis. Dynamic eccentricity fault rotor axis is shifted from the stator axis, the rotor turns around the stator axis. Mixed eccentricity fault rotor turns around the stator axis and rotor axis[17].

To create the effect of static, dynamic, and mixed eccentricity fault in a three-phase PMSM motor. A round pulley of 6 inches in diameter, 2 inches in width, and a four bore of 10 mm in diameter are used to create the fault. The pulley is connected to the shaft to create the eccentricity fault externally without disturbing the motor eccentricity.

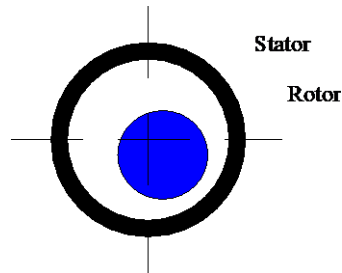


Fig.3 Static eccentricity

Static eccentricity was induced by connecting a balanced load on both sides of the created bore. Dynamic eccentricity was induced by connecting a load on one side of the bore and in mixed eccentricity, an unbalanced load is connected on both sides of the bore.

B. Data Generation and Data acquisition system

For experimentation and data generation the specially designed 1 Hp, three phases, 4 poles, 1500 rpm, and 50 Hz permanent magnet synchronous motor is used.

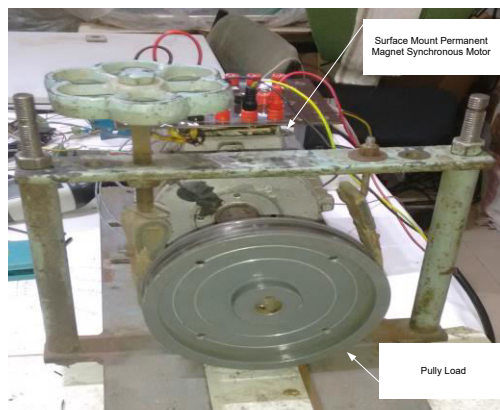


Fig. 4. Experimental Setup

The pulley attached to the belt is used to change the loading conditions of the motor from no load, to rated load, and greater than the rated load.

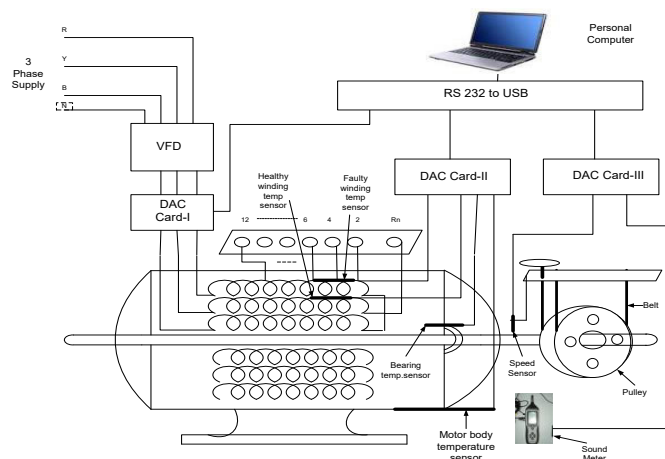


Fig. 5 Process of Experimental setup



Data Acquisition card 1 is used to measure the three-phase motor intake current by using hall effect sensors, three-phase voltage, and power factor. Data Acquisition card 2 is used to measure the temperatures of the motor, healthy winding temperature, faulty winding temperature, bearing temperature, and motor body temperature. Data Acquisition card 3 is used to measure the speed and sound of the motor. All these parameters were recorded with the motor running on no-load, rated load, and greater than rated load for healthy and faulty conditions. with specially designed software in VB 6.0 on a personal computer using RS232 to USB port.

Table 3.Specification of the proposed three-phase PMSM

<i>Item</i>	<i>value</i>
Rated Voltage (Volt)	415
Capacity in hp	1
Pole number	4
Rated speed (rpm)	1500
Rated current (Amp)	1.5
Frequency in (Hz)	50
Total no of slots	24
Turns of the stator winding	500
Length of the stator winding in (mm)	310
Lamination thickness (mm)	0.18
Air gap (mm)	0.6
Coils per phase winding	Double-layer distributed winding
Torque at noload (N-m)	4.78
Torque at Full load (N-m)	5.11
Stator resistance (ohm)	0.0378
Stator inductance (μH)	220
Gauge of winding	21
Double ball bearing	6205ZR
PM flux linkage (wb)	0.0543

C. Data Selection

The first step to designing a neural network is the selection of generated data set. Most relevant data providing fault information should be selected from the generated data set. To avoid the complexity and to improve the classifier performance. In this paper Principal Component Analysis (PCA) is used for the dimensional reduction of the original data set. This technique is a multivariate statistical analysis that can linearly or nonlinearly transform an original set of variables into a significantly smaller set of variables. This technique has been widely used in cluster analysis, pattern recognition, and data compression.

D. Fault Classifier

3. Multilayer Perceptron (MLP) based NN Classifier

Multilayer perceptron (MLPs) are layered feedforward networks typically trained with static backpropagation.[18] These networks have found their way into countless applications requiring static pattern classification.[19] Their main advantage is that they are easy to use and that they can approximate any input and output mapping. As a fault classifier Multilayer perceptron (MLP) neural network is proposed. In the input layer, 12 input PEs are used, and 5 PEs are used in the output layer for five conditions of the PMSM motor namely Healthy condition (H), stator inter-turn (IT), static

eccentricity (SE), dynamic eccentricity (DE) and mixed eccentricity (ME). XLSTAT 2010 and Neuro solution 5.0 are used for data processing.

The randomized data is fed to the neural network and is retained 32 times with different randomized weights to remove the biasing effect and to ensure true learning and generalization for the different hidden layers. It is observed that MLP with a single hidden layer gives better performance. The network is trained with varying PEs in the hidden layer minimum MSE on training and CV is obtained when 18 PEs are used in the hidden layer which is shown in fig.6

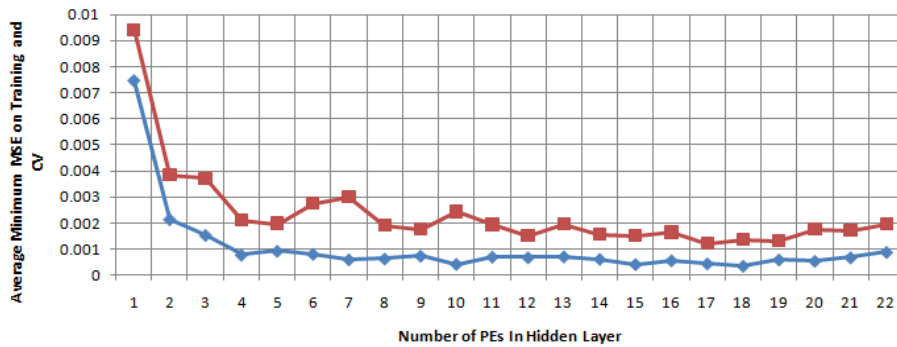


Fig.6 Variation of average minimum MSE on training and cross-validation with the number of PEs in the hidden layer

Various transfer functions and learning are used for training the network. average minimum MSE on training and CV are compared in fig 7(a) and average classification accuracy is compared in fig 7(b). It is found that tanhaxon is the most suitable transfer function and LM is the most suitable learning rule among the various learning rule namely step, Momentum (MOM), conjugate gradient (CG), Levenberg Marquand (LM), Quick propagation (QP) and delta bar delta (DBD) which is shown in fig 8(a) by comparing average minimum MSE on training and CV and in fig 8(b) average classification accuracy is compared.

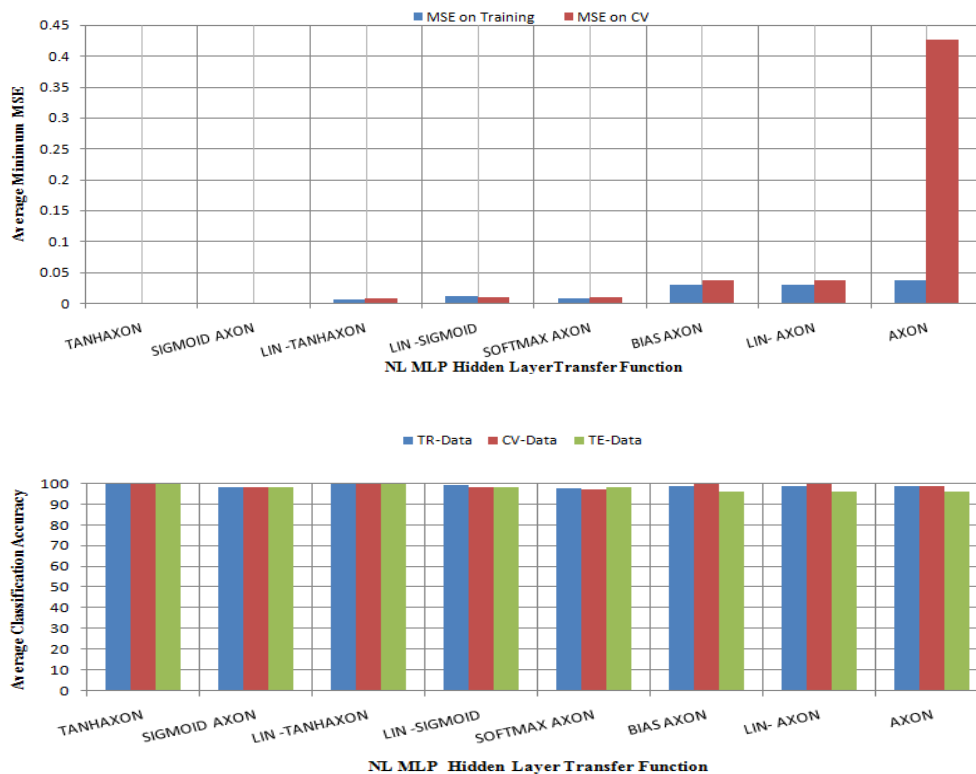


Fig.7 (a) Variation of average minimum MSE on training and cross-validation with hidden layer transfer function (b) Variation of average classification accuracy on training, cross-validation, and testing dataset with hidden layer transfer function

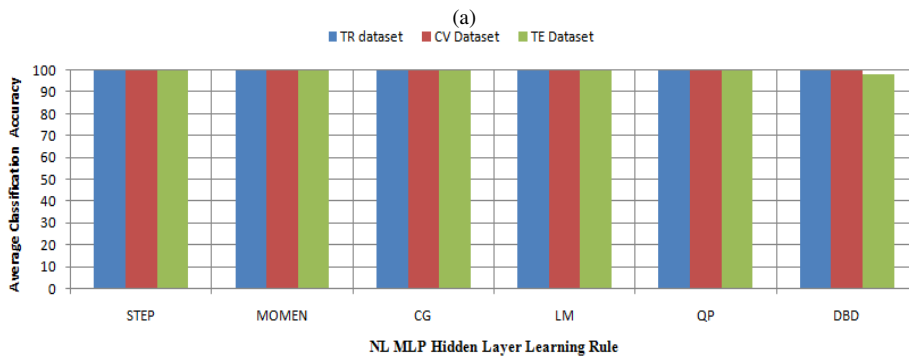
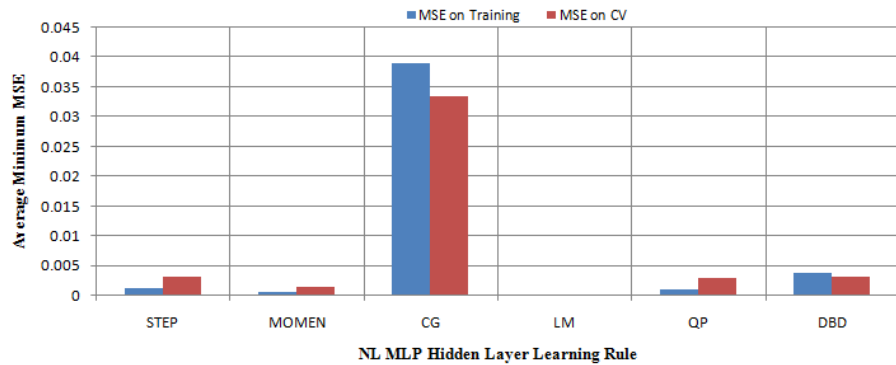


Fig.8 (a) Variation of average minimum MSE on training and cross-validation dataset with hidden learning rule (b) Variation of average classification accuracy on training, cross-validation, and testing dataset with hidden layer Learning rule

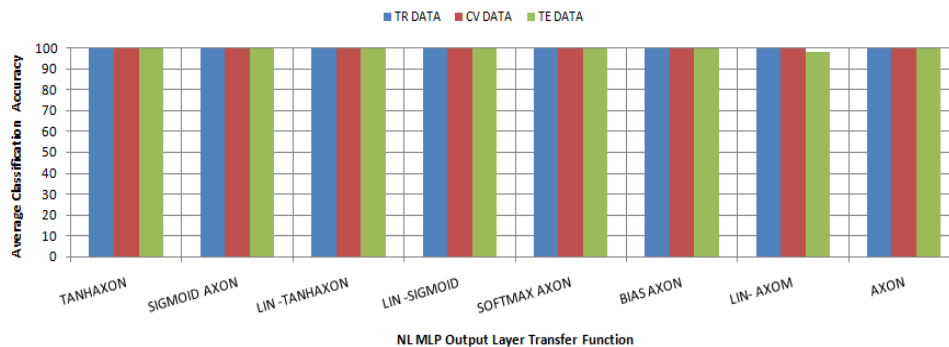
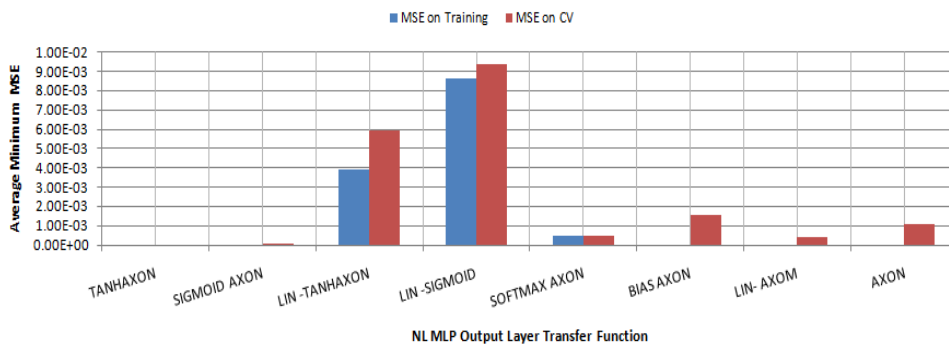


Fig. 9 (a) Variation of average minimum MSE on training and cross-validation dataset with output layer transfer function (b) Variation of average classification accuracy on training, cross-validation, and testing dataset with output layer transfer function

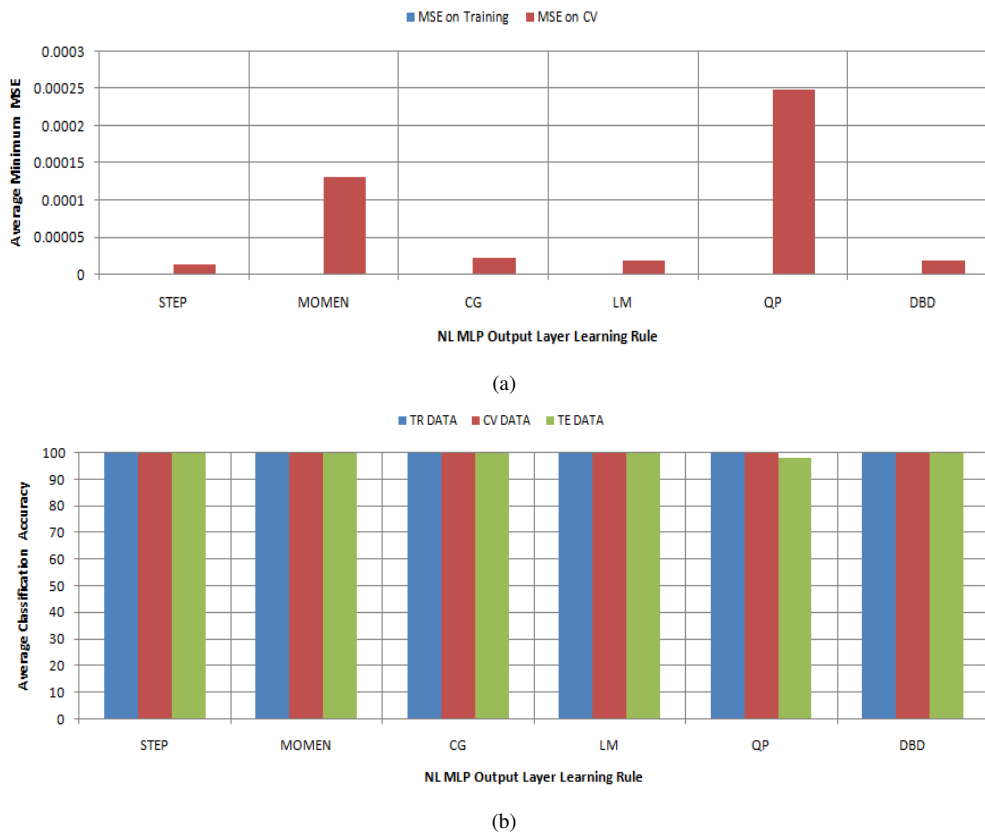
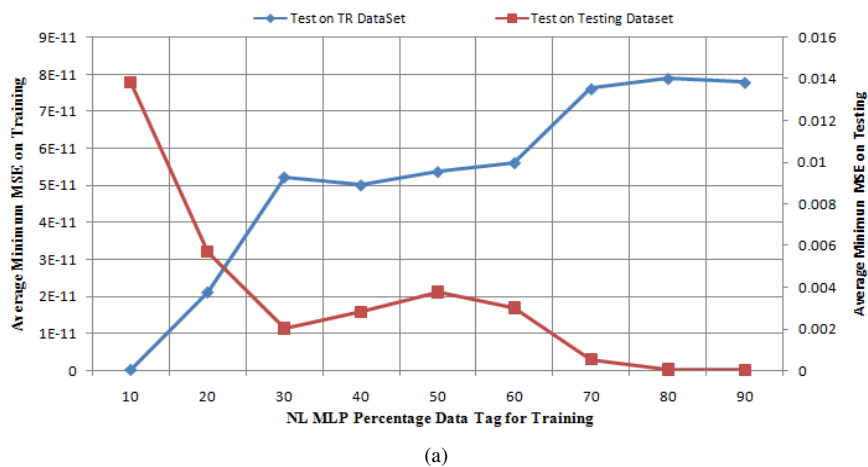
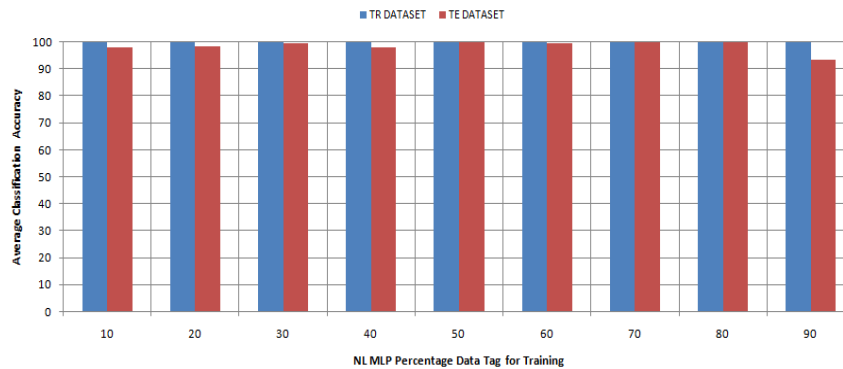


Fig.10 (a) Variation of average minimum MSE on training and cross-validation dataset with output layer learning rule (b) Variation of average classification accuracy on training, cross-validation, and testing dataset with output layer Learning rule

To check the percentage of data tags for training, cv, and testing the network. Various combination of percentage data is used from 10-90 to 90-10. The average minimum MSE on testing and training is shown in fig.11(a) and the average classification accuracy on training and testing is shown in 11(b).

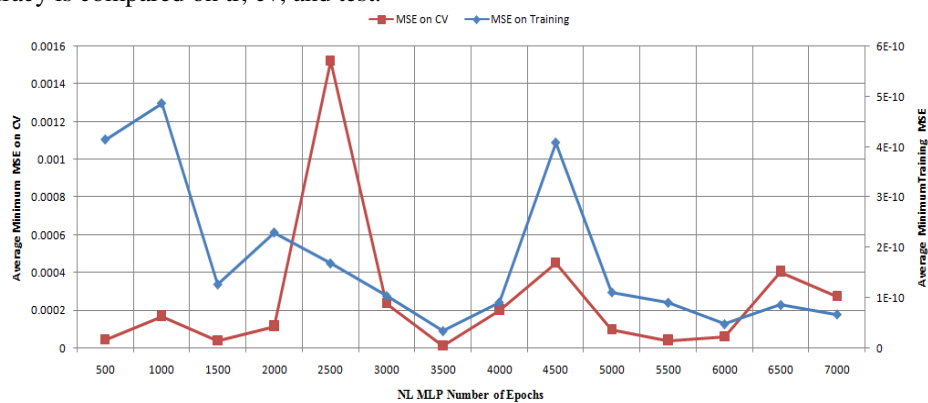




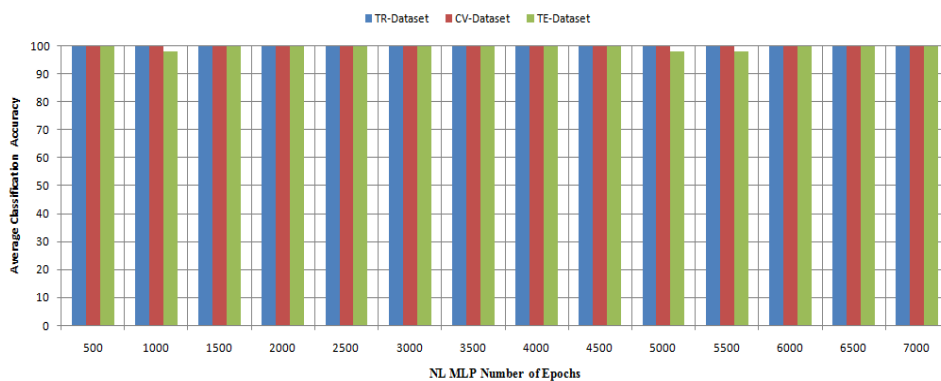
(b)

Fig.11(a) Variation of average minimum MSE with a test on testing and training dataset tagged for tanning (b) Variation of average classification accuracy MSE with the test on testing and training dataset tagged for tanning

The various number of epochs is used for training of network by varying the number of epochs to the small value of epoch 500 to the maximum number of epochs 7000. It is found that at 3500 epochs the best result is obtained which is shown in fig 12(a) by comparing the average minimum MSE on training and CV as shown in fig.12(b) the average classification accuracy is compared on tr, cv, and test.



(a)



(b)

Fig.12 (a) Variation of average minimum MSE on training and cross-validation dataset with Number of epochs (b) Variation of average classification accuracy on training, cross-validation, and testing dataset with number of epochs

With the above experimentation, The MLP-based NN classifier is designed with the following classifications. The number of inputs is 12, the number of hidden layers is 01, the number of PEs in the hidden layer is 18, the number of epochs is 3500, exemplars for training are 70 %, exemplars for cross-validation 15 %, exemplars for testing 15 %. Number of connection weight323, Error criterion L2,



Layers of MLP	Transfer Function	Learning Rule
Hidden	Tanhaxon	LM
Output	Tanhaxon	LM

To check the versatility of the network based on learning ability and classification accuracy. The data is divided into four parts naming 1,2,3, 4, for no load, rated load, and greater than the rated load. Preparing 24 different combinations of group data. Forming 1234,1243 groups likewise. The first two part of the group are tagged as training data, similarly third and fourth part of the group is tagged as cv and testing data. The network is trained and tested on this different combination of data. The average minimum MSE on training and cv is shown in fig 13(a). The average classification accuracy on tr, cv, and test is shown in fig 13(b)

To access the performance of the network for a particular data set, the performance network is used as follows

- (1) Mean Squared Error (MSE)

$$MSE = \frac{\sum_{j=0}^P \sum_{i=0}^N (d_{ij} - y_{ij})^2}{NP}$$

Where,

P= Number of output processing elements

N= Number of exemplars in the dataset

y_{ij} = Network output for exemplar i at processing element j.

d_{ij} = Desired output for exemplar i at processing element j

Normalized Root Mean Squared Error (NRMSE)

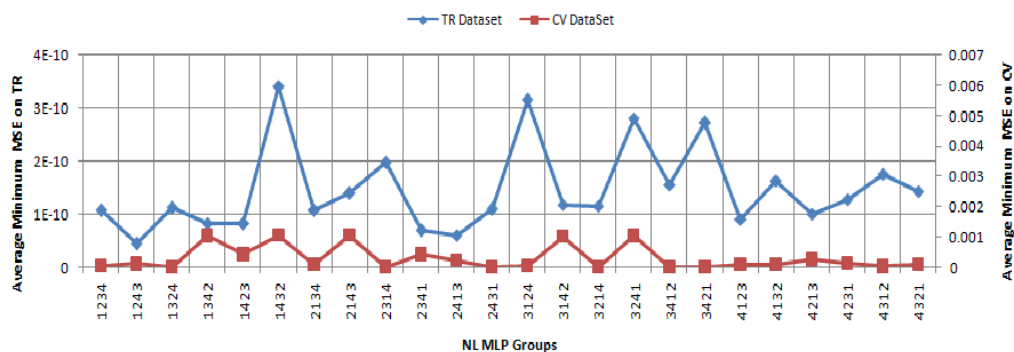
$$NRMSE = \frac{\sqrt{MSE}}{\sum_{j=0}^P \frac{\max(dj) - \min(dj)}{p}}$$

- (2) Mean Absolute Error

$$\% Error = \frac{100}{NP} \sum_{j=0}^P \sum_{i=0}^N \frac{|dy_{ij} - dd_{ij}|}{dd_{ij}}$$

- (3) Correlation coefficient (r)

$$r = \frac{\sum_i (x_i - \bar{x})(d_i - \bar{d}) / N}{\sqrt{\frac{\sum_i (d_i - \bar{d})^2}{N}} \sqrt{\frac{\sum_i (x_i - \bar{x})^2}{N}}}$$



(a)

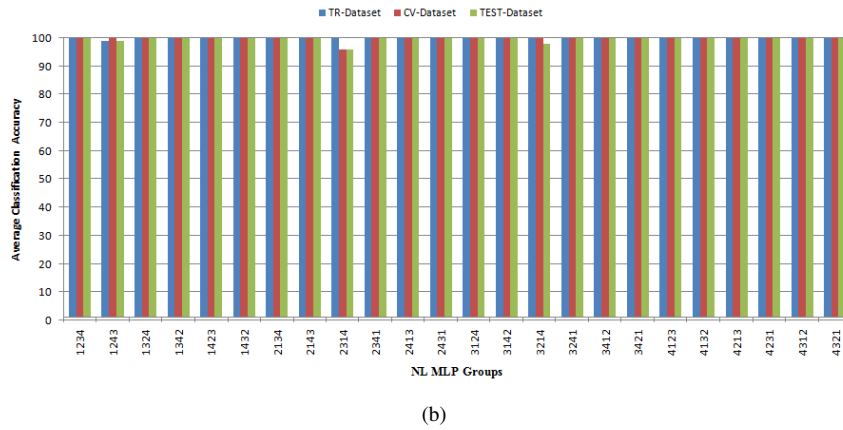


Fig. 13 (a) Variation of average minimum MSE on training and cross-validation dataset with no load group of the dataset (b) Variation of average classification accuracy on training, cross-validation, and testing dataset with no load group of the dataset

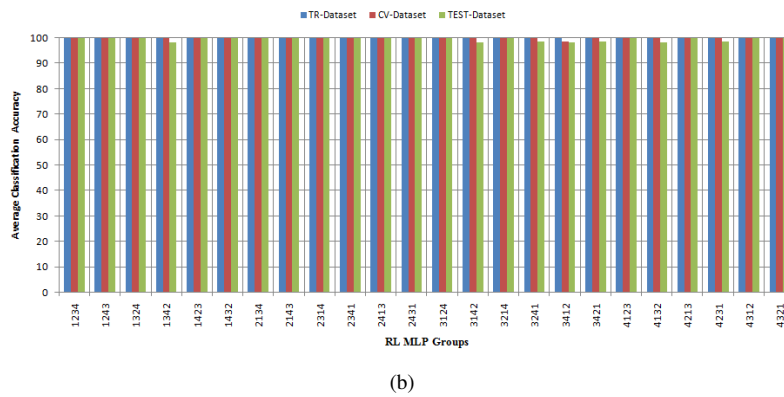
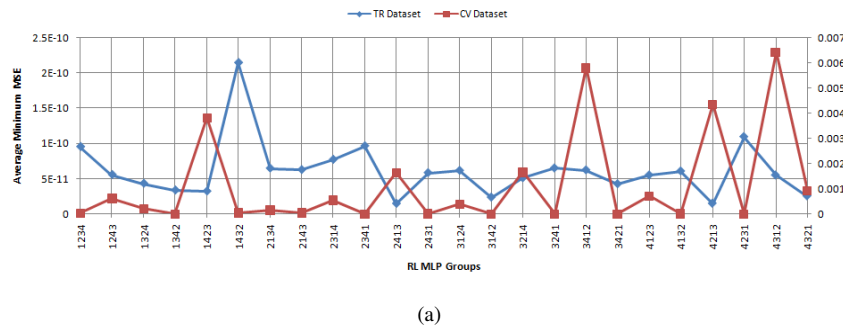
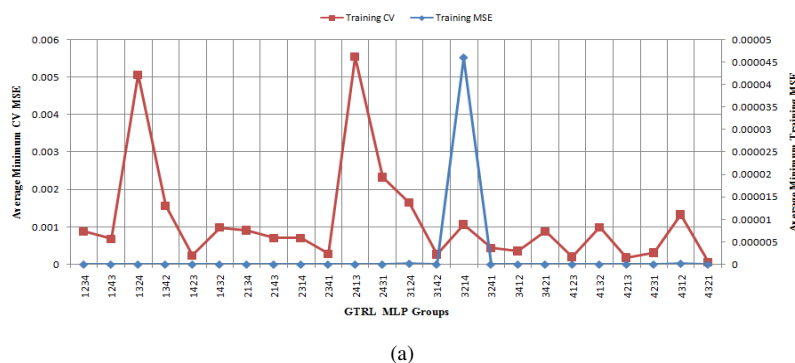


Fig. 14 (a) Variation of average minimum MSE on training and cross-validation dataset with rated load group of the dataset (b) Variation of average classification accuracy on training, cross-validation, and testing dataset with rated load group of the dataset



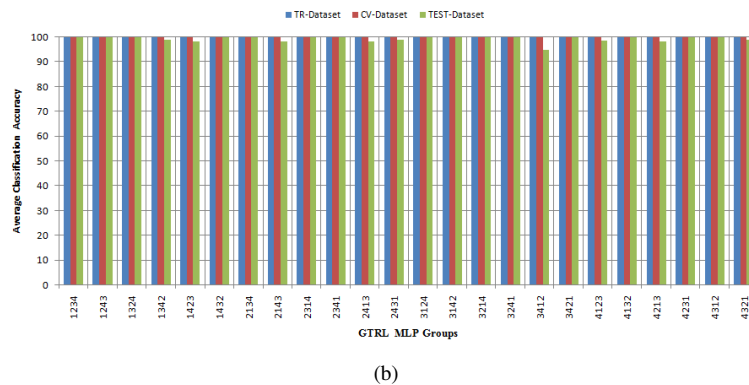


Fig. 15 (a) Variation of average minimum MSE on training and cross-validation dataset with GTRL group of the dataset (b) Variation of average classification accuracy on training, cross-validation, and testing dataset with GTRL group of the dataset

4. Principal component Analysis (PCA) based NN Classifier

A principal component analysis is used for dimensionality reduction of input space input.[20] It is a multivariate statistical technique. Which converts a larger set of correlated or dependent variables to a smaller set of uncorrelated or independent variables is easy to understand and use in future analysis.[21] PCA is performed by the Pearson rule.[22] In this paper, PCA is used along with MLP for the dimensional reduction of 12 statistical input parameters to 5 PCA input parameters. To decide the number of inputs, several PCs are given on each input set, fig 19(a) shows the variation of average minimum MSE on training and CV and fig 19 (b) shows the average classification accuracy on tr, cv, and test datasets. Fig 16 shows the mathematical object, the eigenvalues, which reflects the quality of projection for dimensional reduction of input space. fig.18 shows the correlation circle, from which it is clear that the bearing temperature is closer to the axis therefore it carries information on another axis.

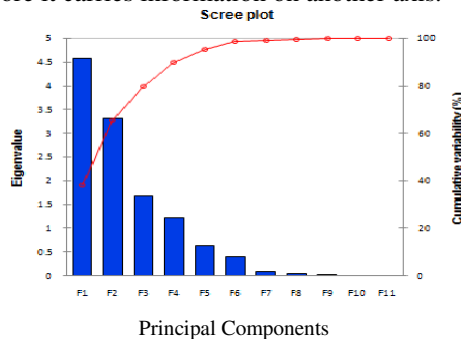


Fig.16 Principal components, Eigenvalues, and percent variability

Table 4. PCA and their variability

Principal Component	Eigenvalue	Variability (%)	Cumulative %
F1	4.580	38.170	38.170
F2	3.312	27.597	65.767
F3	1.681	14.012	79.779
F4	1.222	10.184	89.963
F5	0.634	5.286	95.249
F6	0.398	3.318	98.567
F7	0.090	0.750	99.317
F8	0.041	0.346	99.662
F9	0.023	0.189	99.852
F10	0.012	0.098	99.950
F11	0.006	0.050	100.000

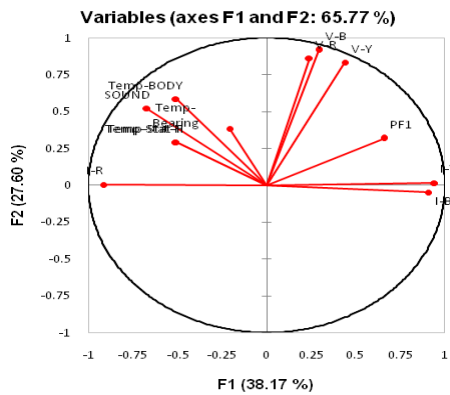


Fig.18 Correlation circle for different statistical parameters and PCs

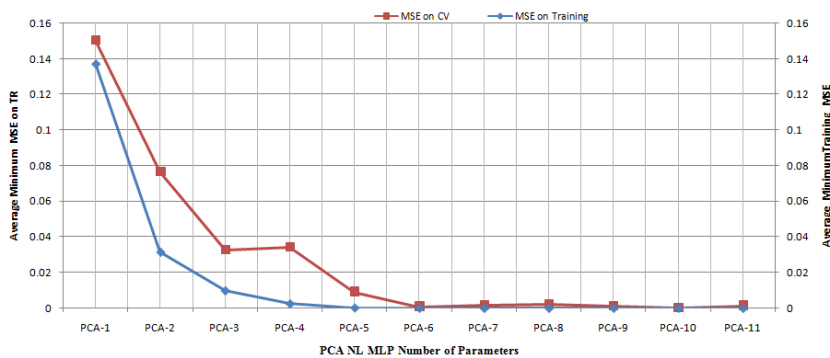


Fig.19 Variation of average minimum MSE on training and cross-validation with number of PCs as input

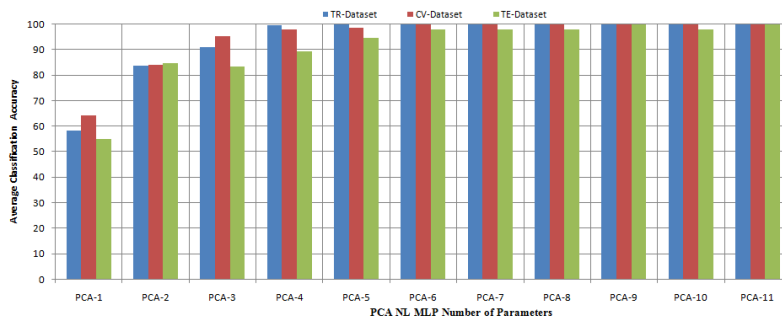


Fig.20. Variation of average classification accuracy on training, cross-validation, and testing dataset with number of PCs as input

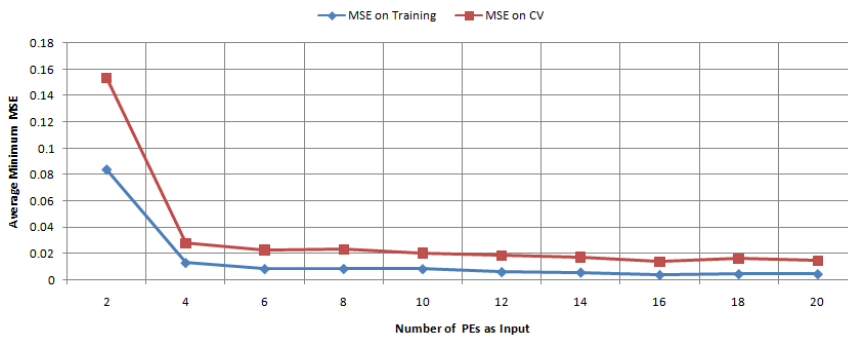
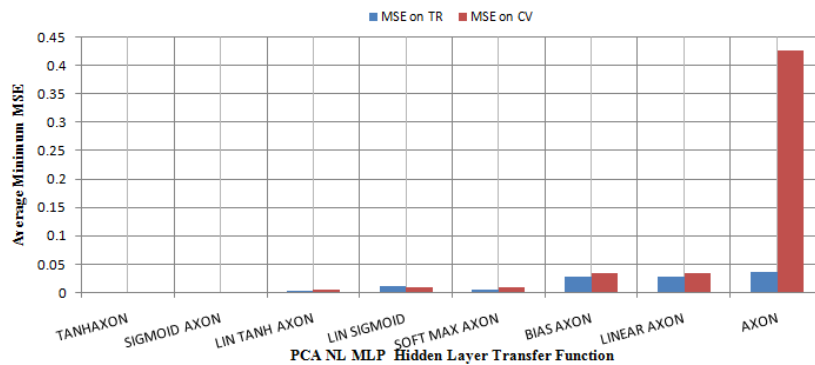
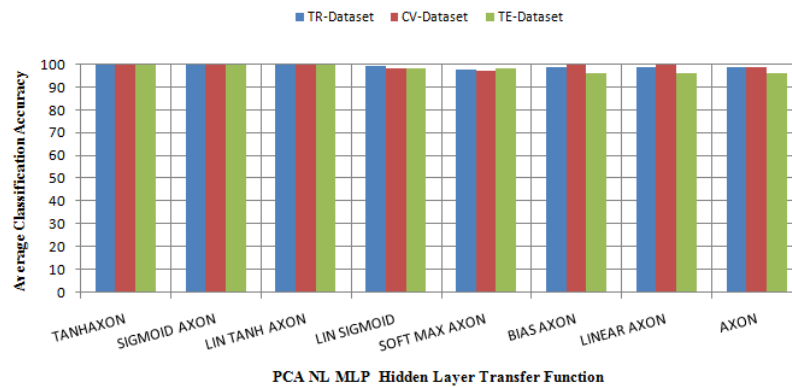


Fig.21 Variation of average minimum MSE on training and cross-validation with number of PEs as input

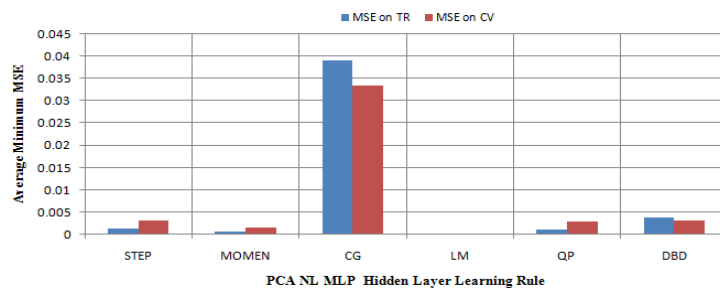


(a)

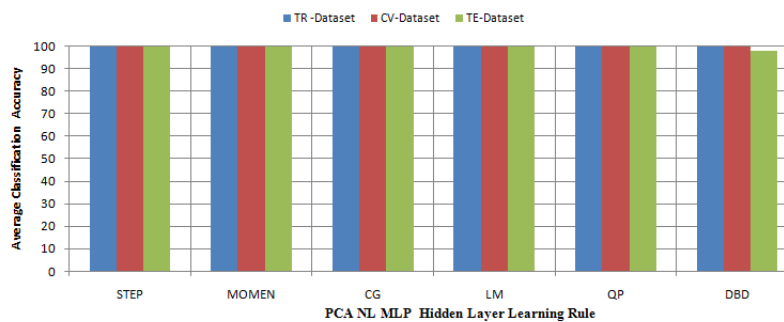


(b)

Fig.22 (a) Variation of average minimum MSE on training and cross-validation dataset with hidden learning rule (b) Variation of average classification accuracy on training, cross-validation, and testing dataset with hidden layer Learning rule

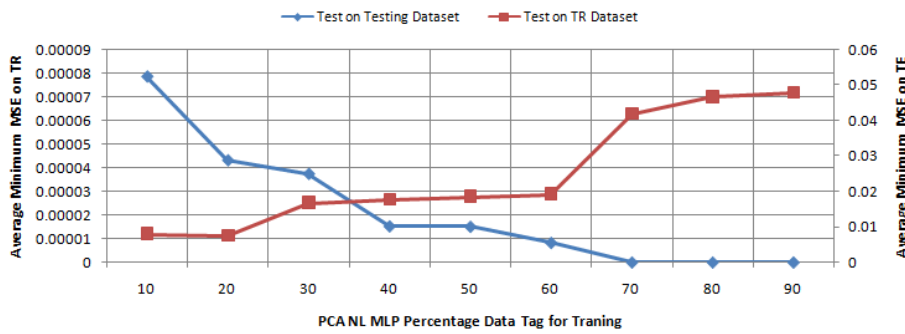


(a)

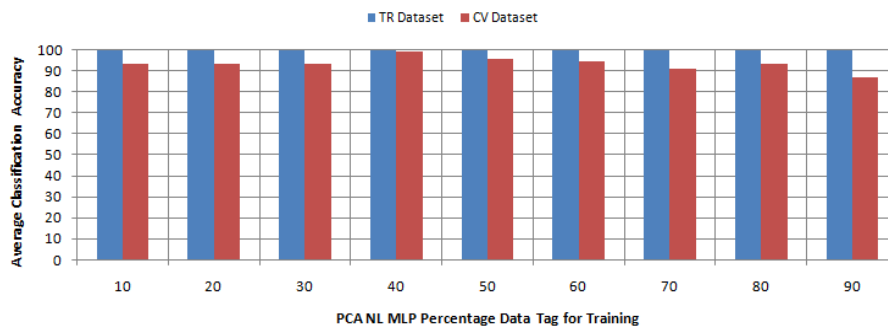


(b)

Fig.23(a) Variation of average minimum MSE on training and cross-validation dataset with output layer transfer function (b) Variation of average classification accuracy on training, cross-validation, and testing dataset with output layer transfer function



(a)



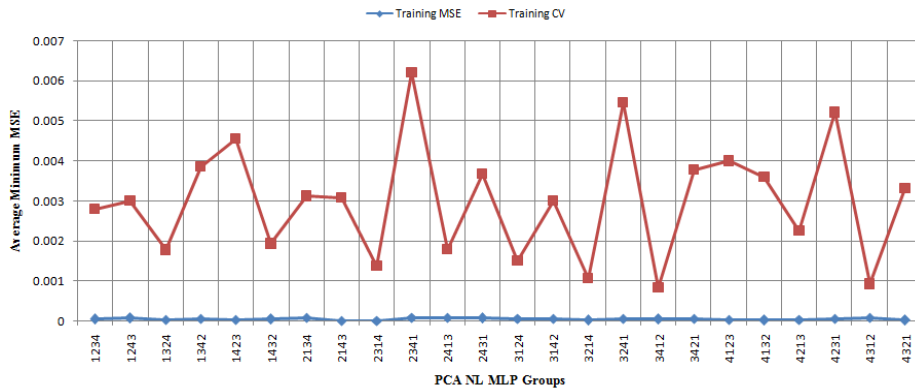
(b)

Fig.24(a) Variation of average minimum MSE with a test on testing and training dataset tagged for training (b) Variation of average classification accuracy MSE with the test on testing and training dataset tagged for training

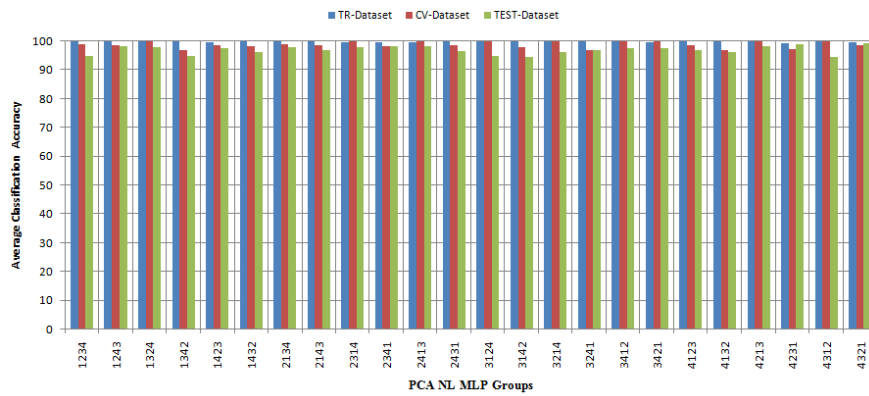
With the above experimentation, The PCA-based NN classifier is designed with the following classifications. The number of inputs is 05, the number of hidden layers is 01, the number of PE in the hidden layer is 16, the number of epochs is 1000, exemplars for training are 70 %, exemplars for cross-validation are 15 %, exemplars for testing 15 %. Number of connection weight 137, Error criterion L2, The network is reduced by 42%.

Layers of MLP	Transfer Function	Learning Rule
Hidden	Sigmoid axon	LM
Output	Sigmoid axon	LM

To check the versatility of the network based on learning ability and classification accuracy. The data is divided into four parts naming 1,2,3, 4.for no load, rated load, and greater than the rated load. Preparing 24 different combinations of group data. Forming 1234,1243 groups likewise. The first two part of the group are tagged as training data, similarly third and fourth part of the group is tagged as cv and testing data. The network is trained and tested on this different combination of data. The average minimum MSE on training and cv is shown in fig 25(a). The average classification accuracy on tr, cv, and test is shown in fig 25(b)

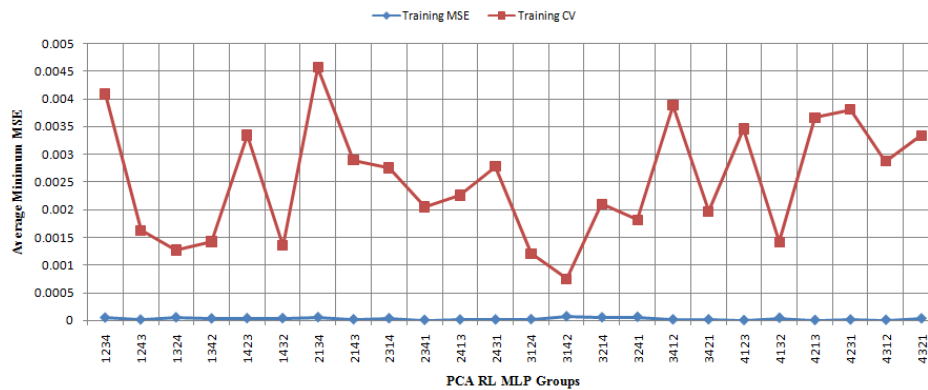


(a)

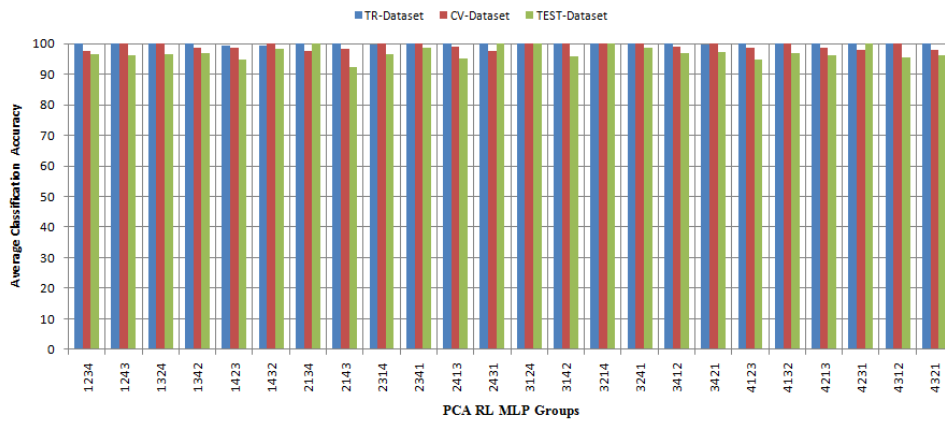


(b)

Fig.25(a) Variation of average minimum MSE on training and cross-validation dataset with no load group of the dataset (b) Variation of average classification accuracy on training, cross-validation, and testing dataset with no load group of the dataset

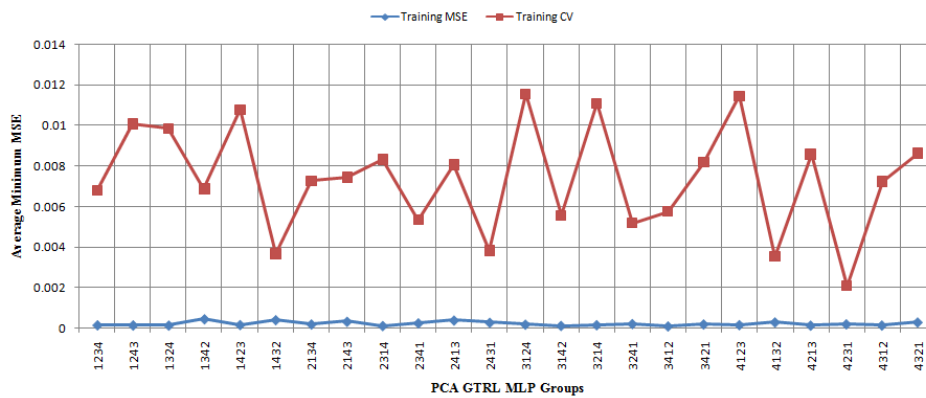


(a)

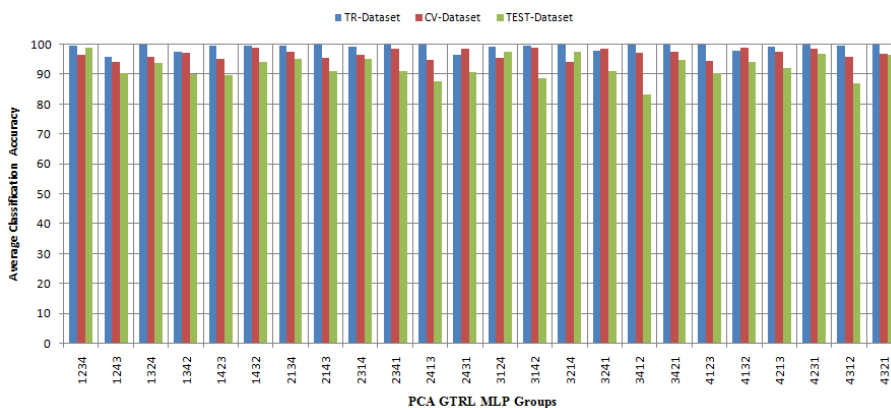


(b)

Fig.26(a) Variation of average minimum MSE on training and cross-validation dataset with rated load group of the dataset (b) Variation of average classification accuracy on training, cross-validation, and testing dataset with rated load group of the dataset



(a)



(b)

Fig.27 (a) Variation of average minimum MSE on training and cross-validation dataset with GTRL group of the dataset (b) Variation of average classification accuracy on training, cross-validation, and testing dataset with GTRL group of the dataset

III. RESULT AND DISCUSION

This paper presents an artificial neural network-based approach for fault detection and classification of a three-phase permanent magnet synchronous motor for two types of incipient faults namely stator inter-turn and eccentricity. An

optimal MLP Neural Network and PCA Neural network are designed and trained to classify different types of faults, stator inter-turn, static eccentricity, dynamic eccentricity, and mixed eccentricity. For MLP NN various transfer functions and learning rules are used for the different numbers of hidden layers and processing elements in the hidden layer. It is observed that tanhaxon transfer function and LM learning rule in the hidden and output layer gives optimum result with 3500 epochs. To check the versatility and learning capability of the network is trained on a different group of the dataset. PCA NN is used for the dimensional reduction of input space from 12 to 5. PCA network with five inputs is designed and trained with various transfer functions and learning rules. It is observed that the sigmoid axon transfer function and LM learning rule gives better optimum result with 1000 epochs. Number of connection weights is reduced by 28% as compared to MLP neural network. From the comparative analysis it is seen that MLP NN (12-18-5) and PCA MLP NN (5-12-5) for the diagnosis of faults in three phase permanent magnet synchronous motor, in the sense that the average MSE on testing and cross validation data set is consistently observed as low as 0.0000725 and 0.000052687 and classification accuracy is obtained as nearly equal to 100%. The classifier is used for real world applications with minor change

REFERENCES

- [1] Bashir Mahdi, Ebrahimi, and Jawad Faiz, "Feature Extraction for Short-Circuit Fault Detection in Permanent-Magnet Synchronous Motors Using In Permanent-Magnet Synchronous Motors Using Stator-Current Monitoring" IEEE Transaction on Power Electronics, Vol.25, NO.10, pp.2673-2682, October 2010.
- [2] M.Hadef, A.Djerdir, M.R.Mekideche, A-O. N'Diaye, Universite de Jijel, "Diagnosis of Stator Winding Short Circuit Faults in a Direct Torque Controlled Interior Permanent Magnet Synchronous Motor" IEEE 2011.
- [3] NicolasLeboeuf, Thierry Boileau, Babak Nahid-Mobarakeh, Guy Clerc And Farid Meibody-Tabar, "Real-Time Detection of Interturn Faults in PM Drives Using Back-EMF Estimation And Residual Analysis" IEEE Transactions On Industry Applications, Vol.47, NO. 6, pp.2402-2412, November/December 2011.
- [4] Luis Romeral, Julio Cesar Urresty, Jordi-Roger Riba Ruiz, Antonio Garcia Espinosa, " Modeling of Surface-Mounted Permanent Magnet Synchronous Motor With Stator Winding Interturn Faults "IEEE Transactions On Industrial Electronics, Vol.58, NO.5, pp1576-1585, May 2011.
- [5] Kyung-Tae Kim, Jun-Kyu Park, JinHur, and Byeong-Woo Kim "Comparison of the Characteristics of IPM-type and SPM-type BLDC Motors Inter-Turn Fault Conditions Using Winding Function Theory", IEEE 2012, pp1262-1269.
- [6] Kyung-Tae Kim, Jun-Kyu Park, JinHur, and Byeong-Woo Kim "Comparison of the Characteristics of IPM-type and SPM-type BLDC Motors Inter-Turn Fault Conditions Using Winding Function Theory" IEEE 2013.
- [7] O.A.Mohammed, Z. Liu, S.Liu, and N. Y.Abed, "Internal Short Circuit Fault Diagnosis For PM Machines Using FE-Based Phase Variable Model And Wavelets Analysis" IEEE Transactions On Magnetics, Vol.43. No.4, pp1729-1732, April 2007
- [8] J.Rosero, L. Romeral, J.A.Ortega, E.Rosero, "Short Circuit Fault Detection In PMSM through Empirical Mode Decomposition (EMD) and Wigner Ville Distribution (WVD)" IEEE 2018, pp98-103.
- [9] Puvan Arumugam, Tahar Hamiti, Chris Gerada, "Analytical modeling of a Vertically Distributed Winding Configuration for Fault-Tolerant Permanent Magnet Machines to Suppress Inter-turn Short Circuit Current Limiting" IEEE 2011, pp371-376.
- [10] Jordi-Roger Riba Ruiz, Javier A.Rosero, Antonio Garcia Espinosa, And Luis Romeral, "Detection of Demagnetization Faults in Permanent-Magnet Synchronous Motors Under Nonstationary Conditions", IEEE Transactions on Magnetics, vol. 45, NO. 7, p.2961-2969, July 2009.
- [11] NicolasLeboeuf, Thierry Boileau, Badak Nahid-Mobarakeh, Nouredine Takorabet, Farid Meibody-Tabar, And Guy Clerc, "Inductance Calculations in Permanent-magnet Motors Under Fault Conditions" IEEE Transactions On Magnetics, Vol. 48, No. 10, p.2605-2616, October 2012.
- [12] BabakVaseghi, Nouredine Takorabet, and faridMeibody-Tabar, "Fault Analysis and Parameter Identification of Permanent-Magnet Motors By Finite-Element Method" IEEE Transactions On Magnetics, Vol. 45, NO. 9, pp 3209-3295, September 2009.
- [13] B.Vaseghi, N.Takorabet, B. Nahid-Mobarakeh, F.Meibody-Tabar, "Modelling and study of PM machines with inter-turn fault dynamic model-FEM model" Electric Power Systems Research 81(2011) pp1715-1722.
- [14] NicolasLeboeuf, Thierry Boileau, Babak Nahid-Mobarakeh, Nouredine Takorabet, Farid Meibody-Tabar, and Guy Clerc, "Estimating Permanent-Magnet Motor parameters Under Inter-Turn Fault Conditions" IEEE Transactions On Magnetics, vol. 48, NO.2, pp 963-966, February 2012.
- [15] Rakib Islam, Mohammad Islam, Joanne Tersigni, Tomy Sebastian, "Inter Winding Short Circuit Fault in Permanent Magnet Synchronous Motors used for High-Performance Applications" IEEE 2012 pp1291-1298.



- [16] J.Urresty, J. Riba, L. Romeral and H. Saavedra, “Analysis of demagnetization Faults in Surface-Mounted Permanent Magnet Synchronous with Inter-turns and Phase-to-Ground Short-Circuits”, IEEE2012, pp2384-2389.
- [17] IlsuJeong, Byong Jo Hyon, And Kwanghee Nam, “Dynamic Modeling and Control for SPMSMs With Internal Turn Short Fault” IEEE Transactions On Power Electronics, Vol. 28, NO. 7, pp3495-3508, July 2013.
- [18] Thierry Boileau, Nicolas Leboeuf, Babak Nahid-Mobarakeh, and Farid Meibody-Tabar, “ Synchronous Demodulation of Control Voltages for Stator Inteturn Fault Detection in PMSM” IEEE Transaction on Power Electronics, Vol. 28, NO. 12, pp5647-5654, December 2013.
- [19] Julio-Cesar Urresty, Jordi-Roger Riba, Luis Romeral. “ Application of the Zero-sequence voltage component to detect stator winding inter-turn faults in PMSMs” Electric Power Systems Research 89(2012), pp38-44.
- [20] Jesus Arellano-Padilla, Mark Sumner and Chris Gerada, “On-Line Detection of Stator Winding Short- Circuit Faults in a PM Machine using HF Signal Injection” Proceedings of the 2008 International Conference on Electrical Machines, pp1-8.
- [21] Dimitri Torregrossa, Amir KHOobroo, and Babak Fahimi, “Prediction of Acoustic Noise and Torque Pulsation in PM Synchronous Machines With Static Eccentricity and Partial Demagnetization Using Field Reconstruction Method”, IEEE Transactions on Industrial Electronics, Vol. 59, NO. 2, pp 934-944, February 2012.
- [22] Bashir Mahdi Ebrahimi, Jawad Faiz, and Mahrsan Javan Roshtkhari, “Static-, Dynamic-, and Mixed-Eccentricity Fault diagnoses in pPermanent-Magnet Synchronous Motor”, IEEE Transaction on Industrial Electronics, Vol. 56, NO.11, pp 4727-4739, November 2009.



INNO SPACE
SJIF Scientific Journal Impact Factor
Impact Factor: 8.118



ISSN INTERNATIONAL
STANDARD
SERIAL
NUMBER
INDIA



INTERNATIONAL JOURNAL OF INNOVATIVE RESEARCH

IN SCIENCE | ENGINEERING | TECHNOLOGY

 **9940 572 462**  **6381 907 438**  **ijirset@gmail.com**



www.ijirset.com

Scan to save the contact details